Microgravity Science and Technology (2018) 30:865–876
https://doi.org/10.1007/s12217-018-9638-1

ORIGINAL ARTICLE

Oscillation Transition Routes of Buoyant-Thermocapillary Convection in Annular Liquid Layers

Longsheng Duan[1,2] · Li Duan[1,2] · Huan Jiang[1,2] · Qi Kang[1,2]

Received: 11 March 2018 / Accepted: 27 June 2018 / Published online: 8 August 2018

Abstract
There are various oscillation transition routes of buoyant-thermocapillary convection in an annular liquid layer. Three types of transition routes including quasi-periodic bifurcation, period-doubling bifurcation and tangent bifurcation have been observed. In our ground experiments, the depth of liquid layer is in a range of 1.6–2.4 mm. The silicone oil with Prandtl number of 28.6 is selected as the liquid medium. The temperature oscillation is detected by a single-point temperature measuring system and the surface oscillation is measured by a laser displacement-sensor with high resolution. The step-heating mode is adopted in the experiments. Transition routes of temperature oscillation and surface oscillation are studied systematically, and the relationship between them is discussed, too.

Keywords Transition route · Buoyant-thermocapillary convection · Bifurcation · Temperature oscillation · Surface oscillation · Step-heating mode

Introduction

Thermocapillary convection is driven by surface tension gradient which is caused by the presence of temperature gradient (Hu and Tang 2003). Czochralski method is one of the main methods to grow monocrystalline materials with high quality and high purity, and the annular liquid pool is the simplified hydrodynamic model of Cz method. On the ground, due to the coupling effect of buoyancy and surface tension, it is difficult to obtain high purity large size crystalline materials and to meet the requirements by high technology industries such as microelectronics industry that needs high quality semiconductor and alloy materials. With the development of manned space technology, the study on crystal growth in the microgravity environment can be realized. Researches conducted in the space station and other space crafts over past decades show that the crystal quality is much better than that obtained by the same method on the ground, even though there are still some defects in the crystal. In the microgravity environment or a small scale flow system, the influence of gravity is greatly weakened, and thermocapillary flow becomes a dominant factor in the natural convection process (Ostrach 1982; Napolitano et al. 1984). Thermocapilly convection in the pool will transform from a steady state to an oscillatory state, which involves a nonlinear instability process and eventually leads to the defects in crystals (Jakeman and Hurle 1972). Therefore, it has a great significance to study the instability mechanism in annular liquid layers. In addition, studies on thermocapillary convection have greatly accelerated the combinations of chaos theory, dissipative structure theory and other disciplines with fluid mechanics, and have greatly enriched the research contents of fluid mechanics.

There are generally three main types of complex structure bifurcations of the nonlinear system in chaotic dynamics: quasi-periodic bifurcation, period-doubling bifurcation and tangent bifurcation (Hale 1991). Gollub and Benson (1980) studied Rayleigh-Bénard convection and found

This article belongs to the Topical Collection: Approaching the Chinese Space Station - Microgravity Research in China
Guest Editors: Jian-Fu Zhao, Shuang-Feng Wang

✉ Li Duan
duanli@imech.ac.cn

✉ Qi Kang
kq@imech.ac.cn

Longsheng Duan
duanlongsheng@imech.ac.cn

[1] Key Laboratory of Microgravity, Institute of Mechanics, Chinese Academy of Sciences, Beijing 100190, China

[2] School of Engineering Science, University of Chinese Academy of Sciences, Beijing 100049, China

four transition routes from laminar flow to turbulent flow. Smith and Davis (1982) conducted research and analyzed the linear stability of thermocapillary convection in an extended liquid layer with a horizontal temperature gradient, and predicted the propagation of hydrothermal waves. Experimental study on thermocapillary instability by Benz et al. (2000) in a rectangular pool with silicon oil as the liquid medium was published, and two kinds of instability that depend on the Bond number of the layer were observed. Numerical study on bifurcation sequences in Rayleigh-Bénard convection was given by Mukutmoni and Yang (1993, 1995). Schwabe et al. (1992) also conducted experimental study on thermocapillary convection in a thin liquid layer. They used the shadowgraph technique to observe the deformation on the gas-liquid interface dynamically. Schwabe et al. (2003) and Sim et al. (2003) reported experimental and numerical results of oscillatory thermocapillary convection in open cylindrical annuli. Short-wavelength and long-wavelength instabilities were observed at two individual situations. Stella and Bucchignani (1999) and Bucchignani and Stella (1999) observed three different bifurcation sequences and obtained two individual mechanisms of the transition to aperiodic oscillations. Numerical results were also reported by Chen et al. (2010) and Li et al. (2010). They found quasi-periodicity and the phase-locking route to the chaotic state. Shi and Imaishi (2006) and Shi et al. (2009) conducted numerical researches on the influence of buoyancy force on thermocapillary convection instability. A counter-intuitive transition route was observed by Yu et al. (2016) and Zhang et al. (2018). They suggested that the spatial complexity of the flow increases as the thermal Marangoni number increases, and it is the reason for the reverse transition from the three-dimensional unsteady flow to the steady flow. Yan et al. (2010) investigated the liquid-bridge model and reported experimental and numerical results of transition processes in thermocapillary convection, and observed the transition route with the period-doubling bifurcation. Yasnou et al. (2018) investigated the influence of a coaxial flow on the evolution of oscillatory states in a liquid bridge. Peng et al. (2011, 2013) observed two types of transition routes of thermocapillary convection in rectangular liquid layers including the period-doubling bifurcation and the quasi-periodic bifurcation, and also studied characteristics of the surface oscillation. Jiang et al. (2017a, b) reported instability of buoyant-thermocapillay convection in open rectangular liquid layers by using a thermal infrared camera. They found that traveling waves would appear on the free surface when $Bd < 1$, and perturbation waves and the surface flow would appear when $Bd >= 1$. They also observed a peculiar bifurcation transition route in the same experimental model, as well as different transition routes with tangent bifurcation to chaos. For an unknown nonlinear system, the chaos theory can be used to explain the transition of fluid state from simple laminar flow to complex turbulent flow.

In this paper, three main modes of oscillation transition are described in both temperature oscillation and surface oscillation. One important finding is that, in the annular liquid layer, the two other bifurcation transition routes are always accompanied by quasi-periodic bifurcation. Besides, the inner relationship between temperature oscillation and surface oscillation is also studied.

Experimental Apparatus

A thermocapillary convection system is established to study the transition routes of temperature oscillations inside the annular liquid layer as well as displacement oscillations on the free surface of the liquid layer. As shown in Fig. 1, the control system of buoyant-thermocapillary convection includes two sets of measuring systems, the temperature measurement system and the displacement measurement system.

As we can see in Fig. 1, the bottom of the circular container is made of K9 optical glass with the thickness of 6 mm. The central column and the outer wall of the circular container are made of the same copper with good thermal conductivity. The radius of the central column (Ri) is 4 mm, the radius of the outer wall (Ro) is 20 mm, and the depth (d) of this circular container is 12 mm. The size effect can be characterized by Ar number, which represents the aspect ratio of the liquid layer: $Ar = h/(Ro-Ri)$, where h is the thickness of the liquid layer. The central column is heated by a resistance heating film, and its temperature is Th. The outer wall is cooled by several peltier elements. Heat is transported outside by means of peltier effect. The temperature on the outer wall is Tc. So the temperature difference $\Delta T = Th - Tc$. Thus, the temperature gradient in the radius direction is established. This experimental model can be used to study thermocapillary convection in liquid layers. Temperatures on the inner column internal as well as on the outer wall are measured by T-type thermocouples and monitored by a Eurotherm 3504 temperature controller. The temperature controller connected with the power supply precisely controls the processes of heating the inner column and cooling the outer wall according to our predetermined program. The temperature measurement system consists of Keithley 2182A Nanovoltmeters and T-type thermocouples. T-type thermocouples can transfer temperature signals into electrical signals so that nanovoltmeters can measure the real-time temperature inside the liquid layer through thermocouples. The temperature measurement range of thermocouples is $-40\ ^\circ C \sim +125\ ^\circ C$. The displacement measurement system contains a Keyence LK-H080 Laser displacement sensor and a LK-HD1500 controller. It

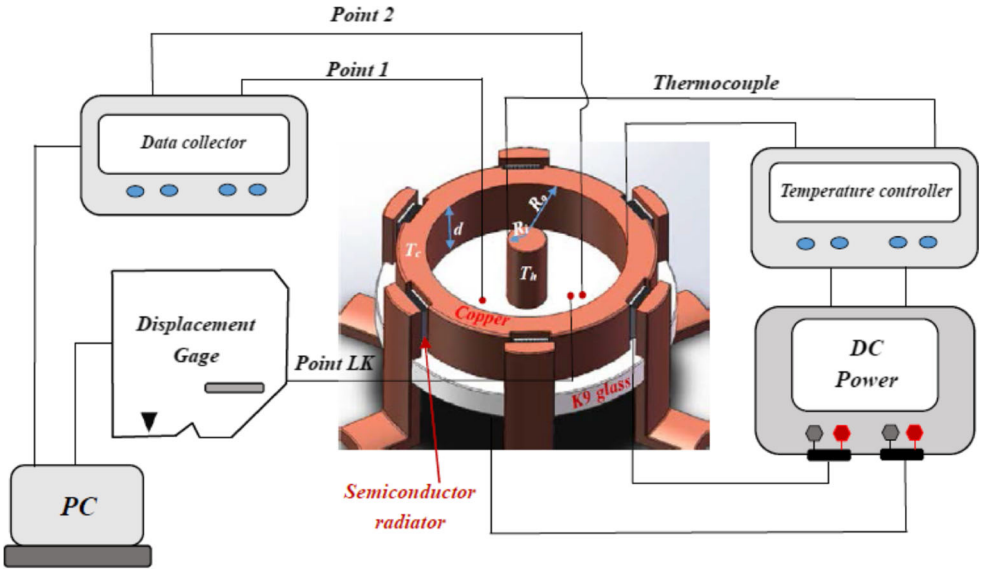

Fig. 1 Control system of buoyant-thermocapillary convection

can measure displacement oscillations on the surface of the liquid layer by using the trigonometry method. The displacement of the target surface can be accurately detected by a laser displacement sensor. The laser triangulation method has characteristics of fast measuring speed, high precision, small measuring point and strong anti-interference ability. The sensitivities of the temperature measurement system and the displacement measurement system are 0.001 °C and 0.1 μm respectively. The sampling frequency in our experiments is 5 Hz. Temperature and displacement signals are collected simultaneously.

Figure 2a shows the locations of temperature measurement points, Point 1 and Point 2 (hereafter referred to as P_1 and P_2), and surface oscillation measurement point Point LK (hereafter referred to as P_L). P_1 and P_L are on the same circumference with radius $R_1 = 12$ mm, and P_2 is on the concentric circle with radius $R_2 = 14$ mm. Figure 2b is the cross-section of the pool. In our experiments, the heads of thermocouples are completely immersed in the pool, and the distance to the bottom of the pool (δ) is 0.5 mm. P_1, P_L and P_2 are in a same diameter. P_1 and P_2 are located at positions in two different areas in the annular fluid layer, so that we can study the relationship between the transition routes of temperature oscillation at two different zones. The locations of P_2 and P_L are close enough for the purpose of investigating similarities and differences in temperature oscillation and surface oscillation between two points in a same region of the annular liquid layer.

In order to study transition routes of oscillations, step-heating mode is adopted in our experiments. The step interval between each temperature difference is 0.5 to 1 °C. The duration of each step is 10 to 15 min. Both the central column and outer wall are equipped with thermocouples, which can accurately feedback temperature signals of hot and cold ends to a temperature controller in real time, so that we can record the temperatures of hot and cold ends in real time Simultaneously, the temperature of the cold end is kept constant by the temperature control system, and the hot end is heated according to preset programs.

The fluid medium used in our experiments is 2cSt silicon oil (Shin-Etsu Chemical Ltd., KF-96). Its physical properties at working temperature are listed in Table 1.

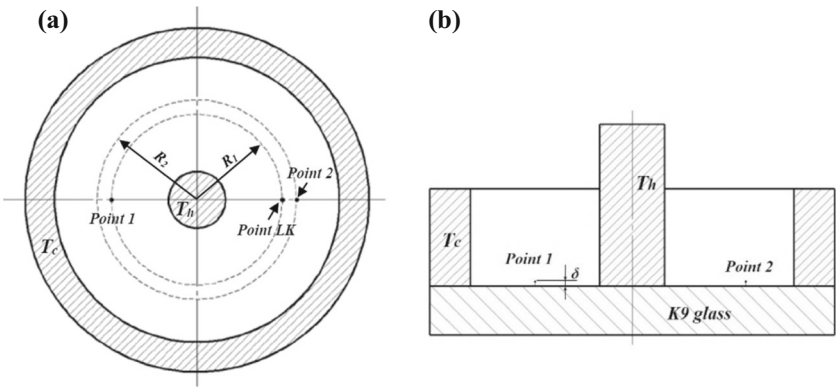

Fig. 2 The locations of temperature and displacement measurement points

Table 1 Physical properties of silicon oil at working temperature (25 °C)

Silicon oil	γ, m^2/s	ρ, kg/m^3	β, 1/°C	κ, m^2/s	σ, N/m	σ_T, N/(m·°C)	Pr
2cSt	2.00×10^{-6}	8.73×10^{2}	1.24×10^{-3}	7.00×10^{-8}	1.83×10^{-2}	-7.15×10^{-5}	28.6

Bond number represents the relative strength of buoyancy to surface tension. Conducting experiments with small Bond numbers is one of the main ways to study thermocapillary convection on the ground. We can carry out experiments with small Bond numbers by changing the scale of the fluid system. $Bd = \frac{\rho g \beta h^2}{(\partial\sigma/\partial T)}$, where ρ is the density, β represents the thermal-expansion coefficient, g is the gravitational acceleration, and $\partial\sigma/\partial$T is the temperature coefficient of surface tension. In our experiments, the range of the thickness of the liquid layer h is from 1.6 mm to 2.4 mm, while the range of Bond number is from 0.397 to 0.893, which indicates that surface tension plays a leading role under the experimental conditions. The Marangoni number, $Ma = \frac{(\partial\sigma/\partial \mathrm{T})\Delta T h}{\mu\alpha}$, can be used to describe the intensity of thermocapillary convection, where $\mu$is the dynamic viscosity and α is the thermal diffusivity.

In this paper, we mainly use the power spectrum method to study characteristics as well as transition routes of oscillations. Power spectrum is the basic tool of studying random vibrations. It can express the statistical properties of stochastic processes on each frequency component. Generally, when describing the randomness of chaotic movements by the power spectrum method, it is assumed that the average amount of oscillation in time is equal to that in space.

Results and Discussions

We find that temperature oscillations and free surface oscillations have same kind of transition routes under the same experimental conditions. In our experiments, there are three main transition routes observed in both temperature oscillations and free surface oscillations.

Transition Routes

The first transition route (hereafter referred to as Route-1) is the quasi-periodic bifurcation sequence. An experiment following this transition route with the liquid layer thickness of 1.6 mm is shown in Fig. 3. The measured temperature data of Point1 is selected for the power spectrum analysis. In addition, the time-frequency spectrum of the temperature oscillation is adopted to study transition processes of thermocapillary convection. Through the time-frequency diagram, we can obtain better information of frequency variations through the whole experiment in detail. Time-frequency diagrams allow us to have a comprehensive understanding of transition routes including possible bifurcation patterns quickly, and when combined with power spectrum analysis afterwards, help us analyze transition routes more accurately. Figure 3e shows the time-frequency spectrum of the temperature oscillation at Point1. The x-coordinate is the frequency, and the y-coordinate is the time. The color in the time-frequency diagram represents the ratio of power to frequency. At the beginning, when the temperature difference between the cold end and the hot end is 28.0 °C and Ma number is 1703, thermocapillary convection starts entering the periodic oscillation state. The fundamental frequency is the one when the oscillation appears for the first time. As shown in Fig. 3a, there is only one frequency, and the fundamental frequency (f_1) is 1.069 Hz. In the time-frequency spectrum of Fig. 3e, we can see the first change in the blue background. Soon after then, when the temperature difference increases to 29 °C and Ma number is 1852, the convection is more intense, and f_1 increases to 1.071 Hz. At this moment, as shown in Fig. 3b, the second fundamental frequency (f_2) appears, $f_2 = 0.9375$ Hz, and the oscillation enters into the quasi-periodic state with two fundamental frequencies. Meanwhile, we can also see the corresponding change in the time-frequency diagram. The two fundamental frequencies f_1 and f_2 are irreducible, and all other frequencies can be expressed by the linear combination of f_1 and f_2. As the temperature difference further increases to 37 °C and Ma number is 2360, $f_1 = 1.221$ Hz, and $f_2 = 1.118$ Hz. Meanwhile, from the time-frequency spectrum of the temperature oscillation, as shown in Fig. 3c, at the location close to where f_1 appears, the third fundamental frequency f_3 (1.187 Hz) appears. The third fundamental frequency f_3 cannot be expressed by the linear combination of f_1 and f_2, while other frequencies can be expressed by the linear combination of these three frequencies. The temperature oscillation transfers from the quasi-periodic state with two fundamental frequencies to the state with three fundamental frequencies. In the time-frequency diagram of Fig. 3e, we can also see the appearance of f_3.

With further increase of the temperature difference, the power spectrum becomes continuous, as shown in Fig. 3d when Ma number is 2808. What we can see in the time-frequency spectrum of the temperature oscillation in Fig. 3e is a bright band and the specific frequencies are unable to be identified clearly. The chaotic movement is bounded and non-periodic, and it can be regarded as the superposition

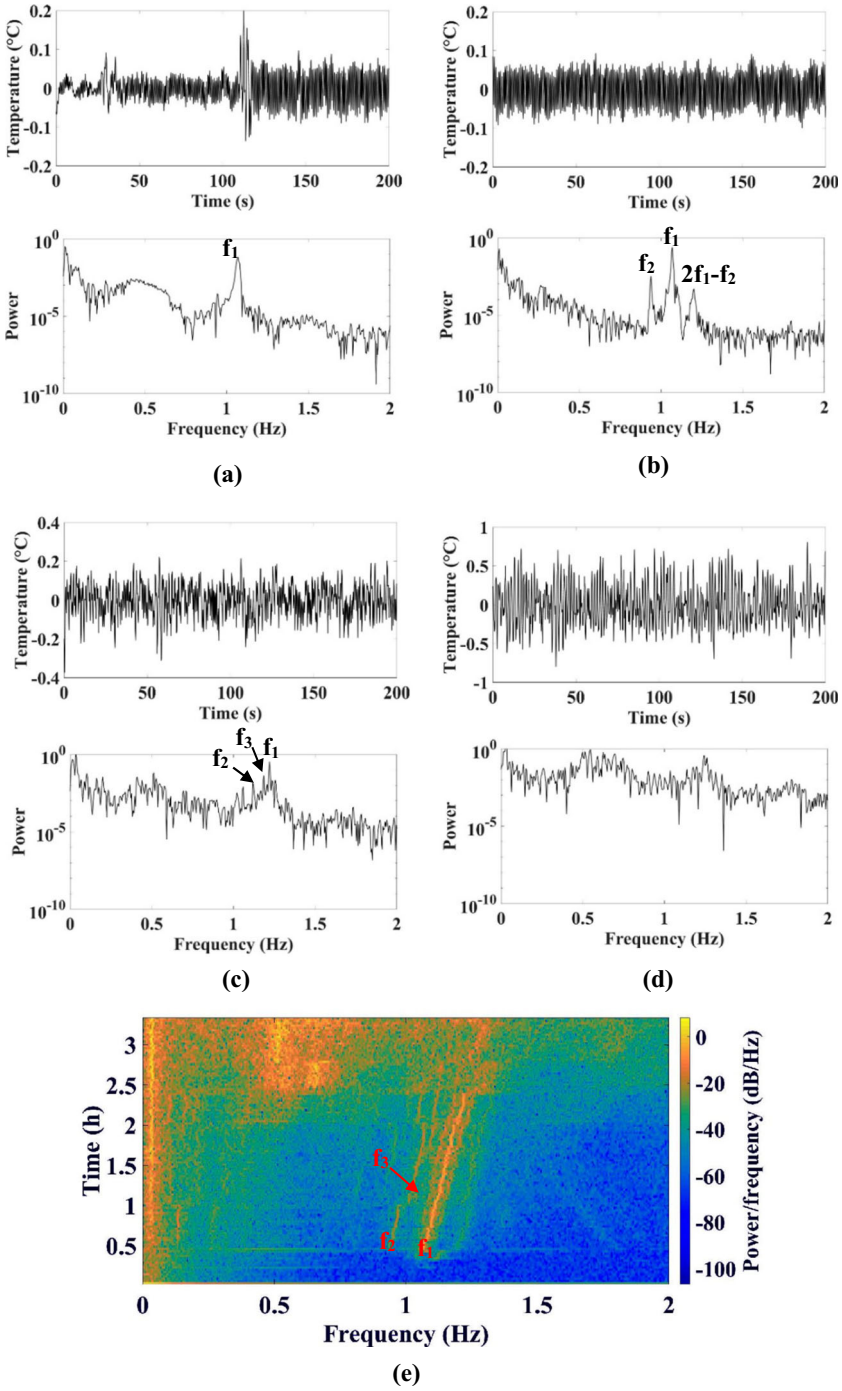

Fig. 3 Time history of temperature oscillations and corresponding power spectra at different Marangoni numbers for Pr = 28.6, h = 1.6 mm and Ar = 0.1: **a** Ma = 1703; **b** Ma = 1852; **c** Ma = 2360; **d** Ma = 2808; **e** Time-frequency spectrum of a temperature oscillation series when Pr = 28.6, h = 1.6 mm and Ar = 0.1

of an infinite number of periodic movements with different frequencies. The power spectrum of chaotic movement is a continuous spectrum with the noise background and the wide peaks It means the oscillation in the annular liquid layer finally transits to the state of aperiodic motion.

At this point, we have obtained a way to enter the chaotic state through two quasi-periodic bifurcation processes, which is consistent with the conclusion obtained by Grebogi et al. (1983) in 1983.

In addition, as shown in Fig. 4, under the experimental condition with h = 2.0 mm and Ar = 0.125, with the increase of Ma, the frequency of these two fundamental frequencies will also increase at the same time and the quasi-periodic bifurcation with two fundamental frequencies will continue. Because small Bond number experiments cannot fully suppress the effect of buoyancy convection, and buoyancy convection and thermocapillary convection will have coupling effect in the annular liquid layer, any

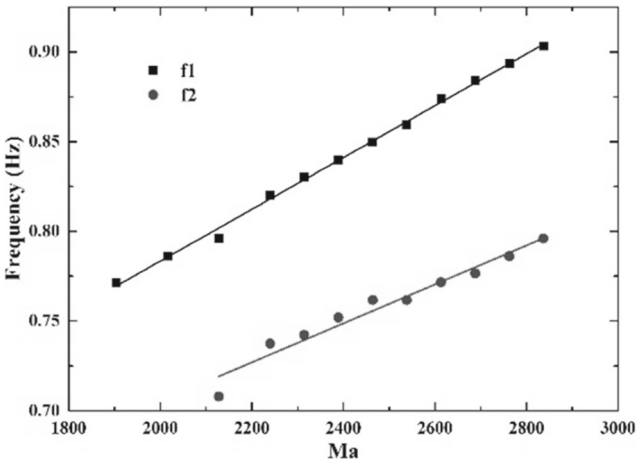

Fig. 4 The fundamental frequencies f_1 and f_2 change with Ma in the flow transition process when Pr = 28.6, h = 2.0 mm and Ar = 0.125

tiny disturbance will cause the transition of the oscillation mode. As the Ma number increases, the convection in the annular liquid layer becomes more intense, leading to the increase in the fundamental frequency of the oscillation and the transition of the oscillation mode.

Meanwhile, we find that there is a special phenomenon in this process: frequency-locking. Frequency-locking refers to the phenomenon that the two characteristic frequencies of the motion of a nonlinear system will be kept as a certain number m/n within a parameter range. As shown in Fig. 5, when the oscillation enters the quasi-periodic bifurcation state, the ratio of f_2 to f_1 will monotone decrease with the increase of Ma except when Ma is in the range of 2300 to 2500. In this range, the ratio of f_2 to f_1 is a constant rational number: 0.895. As shown in Fig. 6, when the number of Ma is in the range of 2300–2500, there is a new frequency f_L in the power spectrum, and f_L satisfies the relationship: $f_L = f_1 - f_2$, and other frequencies in the power

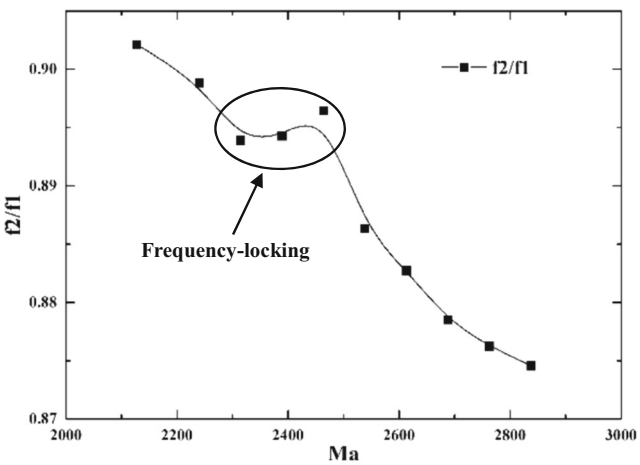

Fig. 5 The ratio of the fundamental frequencies f_2/f_1 changes with Ma in the flow transition when Pr = 28.6, h = 2.0 mm and Ar = 0.125

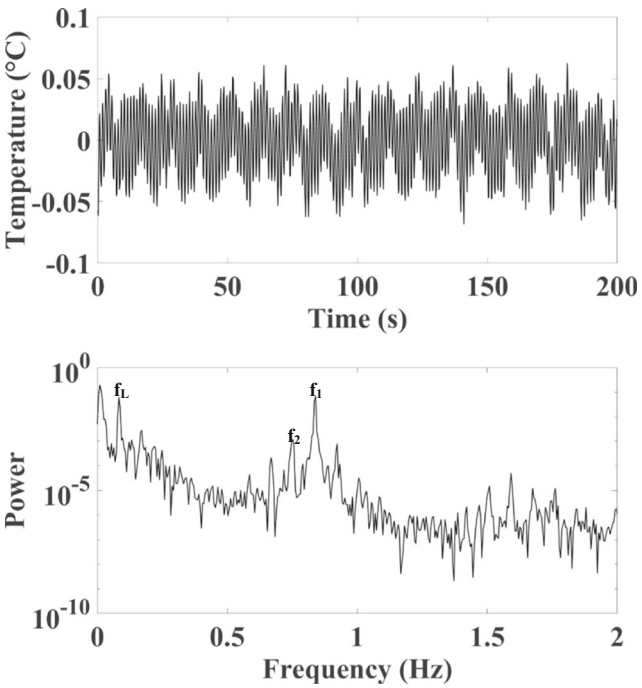

Fig. 6 The power spectrum at Ma = 2400, Pr = 28.6, h = 2.0 mm and Ar = 0.125

spectrum are multiples of f_L. At this time, the convection is oscillating periodically with frequency f_L. Figure 6 shows the typical characteristics of the power spectrum. When the frequency-locking phenomenon occurs, f_1 = 0.9277 Hz, f_2 = 0.8398 Hz, and f_L = 0.088 Hz ($f_1 - f_2$). Similar frequency-locking phenomenon also exists in the surface oscillation under the same experimental condition.

The second transition route (hereafter referred to as Route-2) is the period-doubling bifurcation accompanied with quasi-periodic bifurcations. This transition route can be identified under the experimental conditions with h = 2.4 mm and Ar = 0.15, as shown in Fig. 7. During the initial period of the experiment, the transition route of thermocapillary convection follows the quasi-periodic bifurcation sequence: the periodic oscillation state in Fig. 7a (f_1 = 0.5225)—the quasi-periodic oscillation state with two fundamental frequencies in Fig. 7b (f_1 = 0.5332 and f2 = 0.5762)—the quasi-periodic state with three fundamental frequencies in Fig. 7c. When the temperature difference is 37 °C and Ma = 3315, the fundamental frequencies of oscillation are f_1 = 0.581 Hz, f_2 = 0.625 Hz and f_3 = 0.547 Hz. In Fig. 7d (Ma = 3315), A frequency equal to one half of the fundamental frequency (1/2 f_1 = 0.291 Hz) appears in the power spectrum, which indicates that thermocapillary convection has entered into the period-doubling bifurcation state. However, the period-doubling bifurcation state is not stable. Then it will transit to the quasi-periodic bifurcation state again, as shown in Fig. 7e

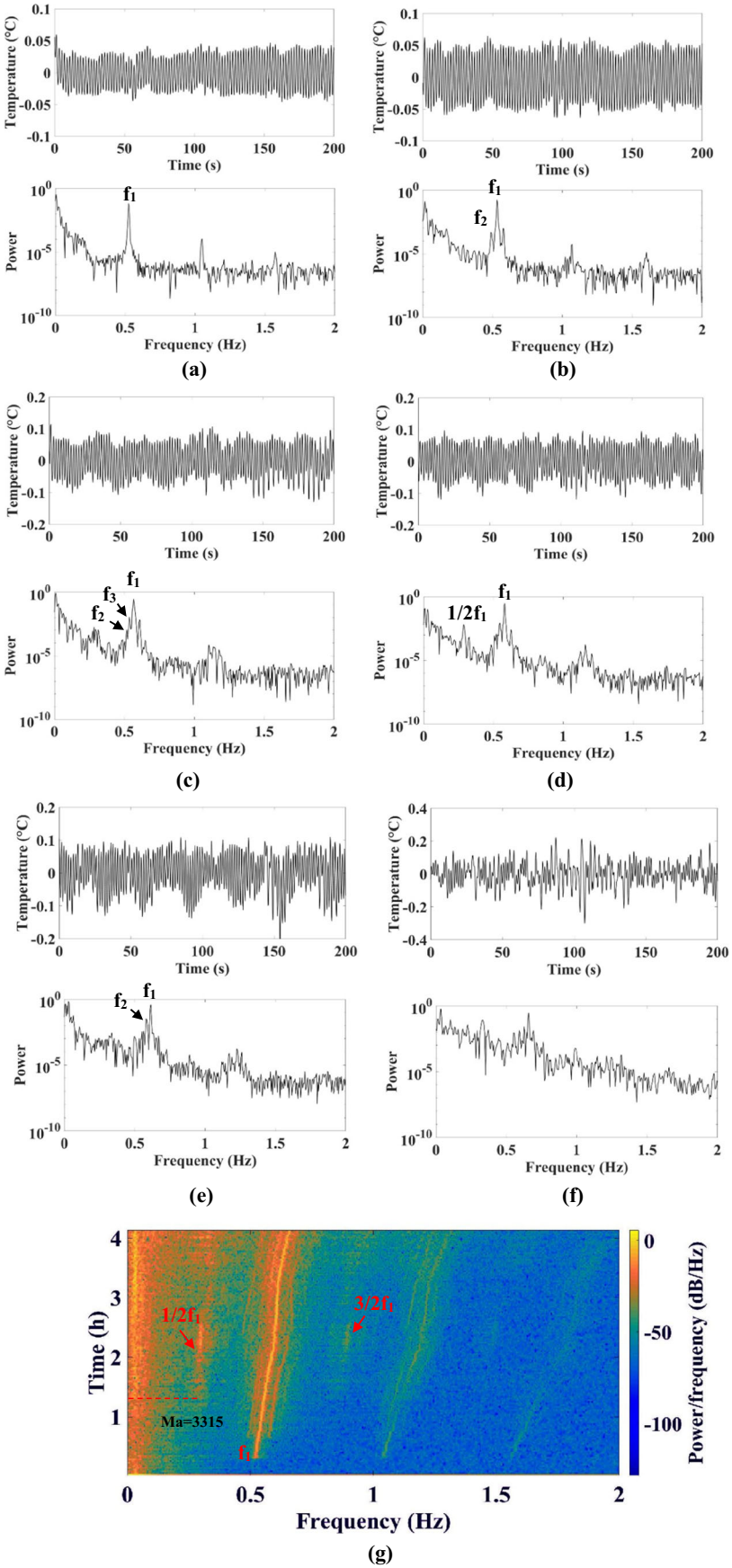

Fig. 7 Time histories of temperature oscillations and corresponding power spectra at different Marangoni numbers with Pr = 28.6, h = 2.4 mm and Ar = 0.15: **a** Ma = 2464; **b** Ma = 2643; **c** Ma = 3136; **d** Ma = 3315; **e** Ma = 3719; **f** Ma = 4032; **g** Time-frequency spectrum of a temperature oscillation series when Pr = 28.6, h = 2.4 mm and Ar = 0.15

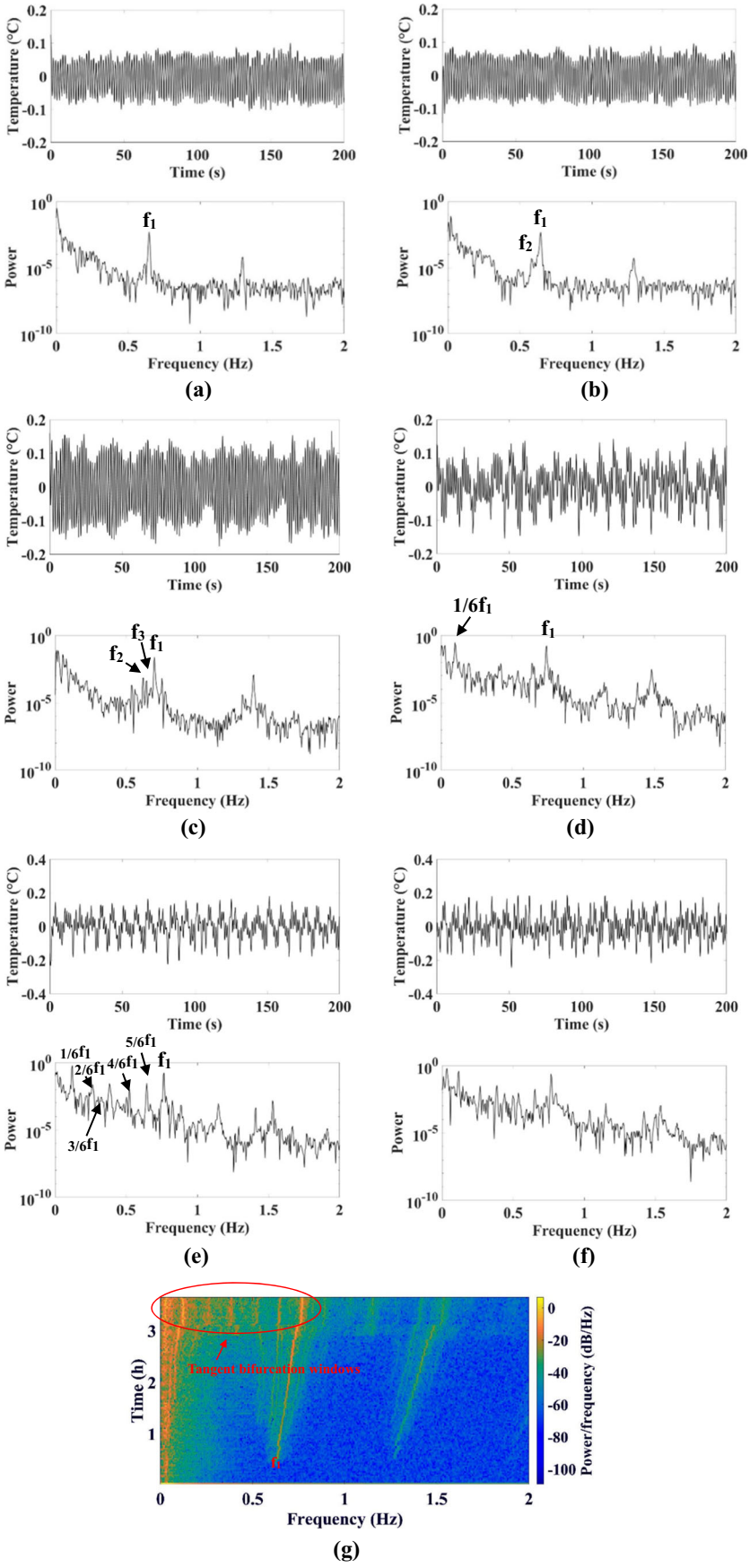

Fig. 8 Time histories of temperature oscillations and corresponding power spectra at different Marangoni numbers with Pr = 28.6, h = 2.2 mm and Ar = 0.1375: **a** Ma = 2299; **b** Ma = 2381; **c** Ma = 3039; **d** Ma = 3450; **e** Ma = 3532; **f** Ma = 4011; **g** Time-frequency spectrum of temperature oscillation when Pr = 28.6, h = 2.2 mm and Ar = 0.1375

(Ma = 3719), and finally to the aperiodic oscillation state, as shown in Fig. 7f

In Fig. 7g, we can also see clearly that when Ma = 3315, the frequency of half of the fundamental frequency, 1/2 f_1, appears. Compared with our previous investigations in the period-doubling bifurcation transition route in a rectangular liquid layer (Peng et al. 2013), the period-doubling transition route in the annular liquid layer is different. As the period-doubling bifurcation of temperature oscillation appears with the frequency of 1/2 f_1, the oscillation won't further bifurcate into the period-doubling state with the frequency of a quarter of f_1, but transit to the quasi-periodic bifurcation state again. So, in the process of the period-doubling bifurcation, it is also accompanied with the quasi-periodic bifurcation. These two kinds of bifurcations work together, and oscillations in thermocapillary convection do not simply follow the period-doubling transition route.

The third transition route (hereafter referred to as Route-3) is the tangent bifurcation accompanied with quasi-periodic bifurcations. When an odd number of bifurcations occur, it is called the tangent bifurcation (Delbourgo and Kenny 1985; Broze and Hussain 1996). In the transition process of thermocapillary convection in the annular liquid layer, the tangent bifurcation is extremely unstable. Only under the experimental condition with h = 2.2 mm and Ar = 0.1375, can we observe the tangent bifurcation clearly. The transition route with the tangent bifurcation is also along with quasi-periodic bifurcations. As shown in Fig. 8, the transition route of tangent bifurcation follows the same sequence as the period-doubling bifurcation route during the initial period of the experiment: the periodic oscillation state in Fig. 8a (Ma = 2299, and f_1 = 0.6445)—the quasi-periodic oscillation state with two fundamental frequencies in Fig. 8b (Ma = 2381, f_1 = 0.6496 and f2 = 0.6201)—the quasi-periodic state with three fundamental frequencies in Fig. 8c (Ma = 3039, f_1 = 0.6982, f_2 = 0.6445 and f_3 = 0.6201). As shown in Fig. 8d, when the temperature difference is 41 °C and Ma is 3450, there is a harmonic with the frequency of one sixth of the fundamental frequency in the power spectrum (1/6 f_1). At this time, f_1 is 0.7422 Hz and 1/6 f_1 is 0.122 Hz. As the temperature difference increases to 43 °C and Ma is 3532, sub-harmonics with frequencies from 1/6 f_1 to 5/6 f_1 can be identified in Fig. 8e. We can see a very clear tangent bifurcation window in the time-frequency spectrum of the temperature oscillation in Fig. 8g. Table 2 lists the relationship between the fundamental frequency and other frequencies of the sub-harmonics. Due to the limitation of experimental conditions, the max temperature difference between the cold end and the hot end is 50 °C and Ma is 4011, and the stable temperature difference step at a higher temperature is hardly to achieve. As shown in Fig. 8f, the temperature oscillation is still in the state with tangent bifurcations. However, since the tangent bifurcation is an unstable oscillation mode, it will eventually transit to the quasi-periodic oscillation state and finally reach the chaotic state.

As mentioned above, thermocapillary convection in the annular liquid layer will transit from the periodic oscillation state to the quasi-periodic oscillation state quickly. The temperature data measured by the thermocouple located at P_2 under five sets of experimental conditions is analyzed to study transition processes from periodic state to quasi-periodic state. The critical Ma numbers of periodic and quasi-periodic oscillations are shown in Fig. 9. The difference in Ma number between these two states is in the range of 100–125, which means that thermocapillary convection will transfer from periodic state to quasi-periodic state quickly. This is due to the effect of buoyancy convection. The existence of buoyancy in the annular liquid layer causes the convection along the vertical direction and disturbs the relatively stable temperature distribution, and finally leads to the rapid transition of temperature oscillation from a relatively stable periodic oscillation state to a more complex quasi-periodic oscillation state.

The Relationship Between Transition Routes of Temperature Oscillation and Surface Oscillation

In our experiments, there are also three types of transition routes in the free surface oscillation. It is because that temperature oscillation and free surface oscillation are two different forms of the same oscillation in the annular liquid layer. We can investigate the similarities and differences between temperature oscillation and surface oscillation through P_2 and P_L, and study the relationship between the transition routes of temperature oscillation at two different measurement points in the annular liquid layer through P_1 and P_2.

Table 2 The relationship between the fundamental frequency and frequencies of other sub-harmonics at different Marangoni numbers under the experimental condition with Pr = 28.6 and h = 2.2 mm

	The periodic bifurcation	The period-sextupling bifurcation
Ma	2299	3532
The fundamental frequency (Hz)	0.6445(f_1)	0.7666(f_1)
Other frequencies of sub-harmonics (Hz)	1.29($2f_1$)	0.127($1/6f_1$); 0.26($2/6f_1$); 0.3809($3/6f_1$); 0.521($4/6f_1$); 0.639 ($5/6f_1$);

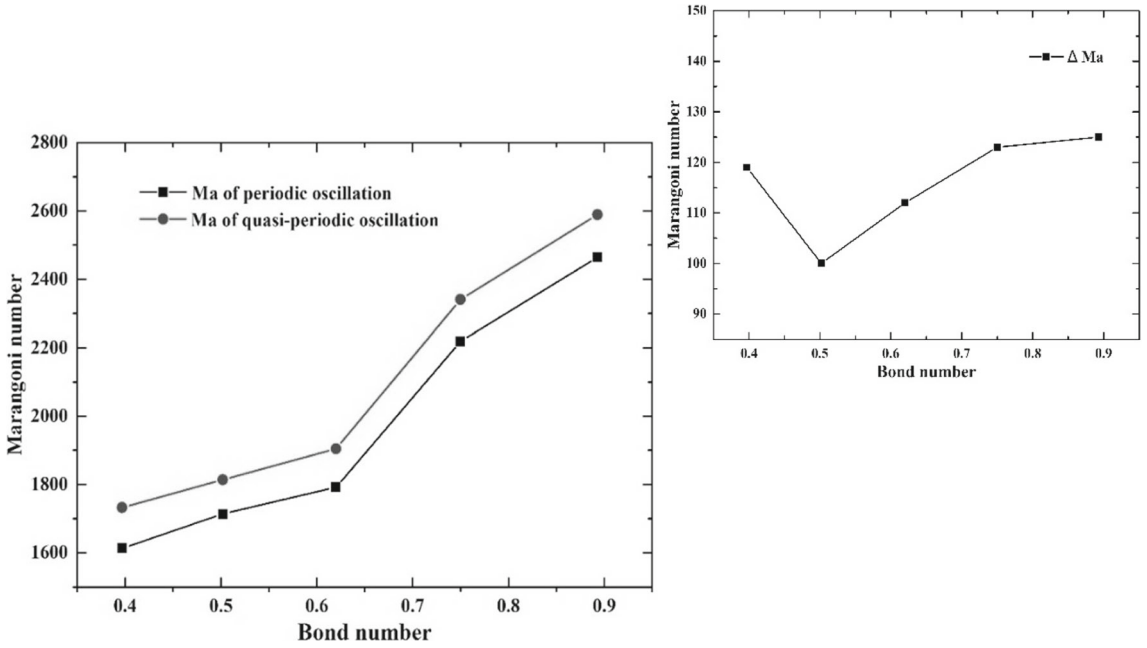

Fig. 9 The critical Ma numbers of periodic and quasi-periodic oscillations

Figure 10 shows the time-frequency spectra of temperature oscillations and free surface oscillations at P_1, P_2 and P_L. The corresponding experimental conditions for each row are h = 1.8 mm (Ar = 0.1125), h = 2.4 mm (Ar = 0.15) and h = 2.2 mm (Ar = 0.1375) respectively. By observing these time-frequency spectra of surface oscillations, it

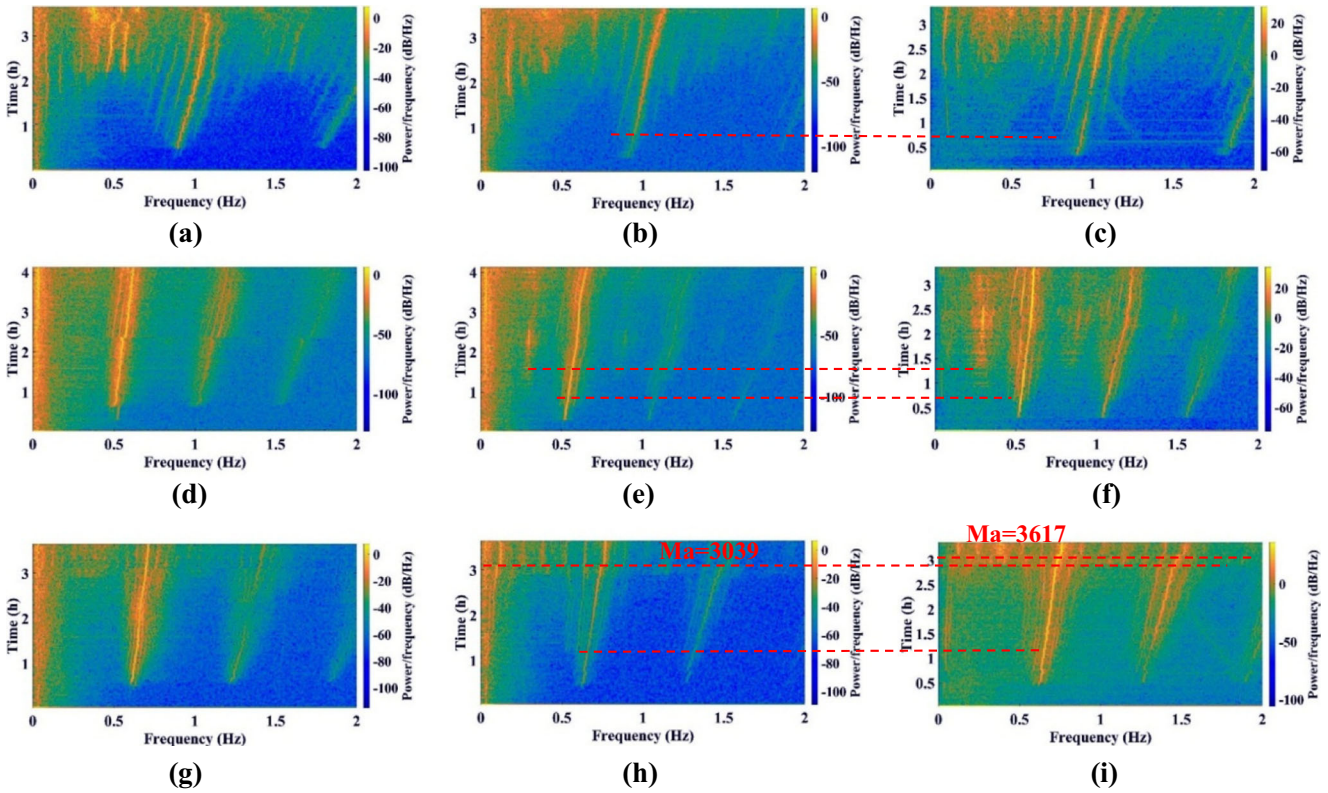

Fig. 10 The time-frequency spectra of temperature oscillations and surface oscillations at the temperature measurement points (P_1 & P_2) and the surface oscillation measurement points (P_L): P_1: (**a**), (**d**), (**g**); P_2: (**b**), (**e**), (**g**); P_L: (**c**), (**f**), (**i**)

is easy to find that there are also three transition routes in the displacement oscillation. As shown in Fig. 10c, the quasi-periodic bifurcation sequence of the surface oscillation can be obtained when Ar is 0.1125. A process with a period-doubling bifurcation when Ar is 0.15 and a process with a tangent bifurcation when Ar is 0.1375 are shown in Fig. 10f and i respectively. It can be seen from the time-frequency diagrams that the temperature oscillation and the surface oscillation have similar transition routes, therefore, it can be concluded that the transition route of the displacement oscillation is consistent with that of the temperature oscillation in the same region of the liquid layer. By comparing time-frequency diagrams of temperature oscillations and free surface oscillations and investigating the time nodes of bifurcation transitions, we find that, when the transition follows Route-1 or Route-2, the time nodes of bifurcations in the temperature oscillation are consistent with that in the corresponding transition of the surface oscillation. However, when the transition route follows Route-3, the distinct difference appears. When Ma = 3039, the temperature oscillation has transferred from the quasi-periodic bifurcation state to the tangent bifurcation state, but the surface oscillation is still in the quasi-periodic oscillation state, and until when Ma = 3617, the surface oscillation just enters into the tangent bifurcation state. The reason is that both of the quasi-periodic bifurcation and the period-doubling bifurcation are relatively stable bifurcation forms, so the temperature oscillation is consistent with the displacement oscillation in Route-1 (Fig. 10b, c) and Route-2 (Fig. 10e, f). However, the tangent bifurcation is a very unstable form and the time nodes of the tangent bifurcation are random, therefore, there is a time difference by comparing time-frequency spectra in Fig. 10h and i. More profound mechanisms will be further explored in our follow-up studies.

Besides, the time-frequency spectra of P_1 & P_2 under three experimental conditions are compared by same methods. In Fig. 10a and b, we can see that the transitions of temperature oscillations at these two points follow Route-1. It indicates that two points in different regions of the annular liquid layer share the same oscillation transition path. There are also some differences in their temperature oscillation modes. Figure 10g shows the quasi-periodic evolution process. Figure 10h shows the obvious process of the tangent bifurcation in the time-frequency spectrum of P_2 when Ar is 0.1375. Compared with the time-frequency spectrum in Fig. 10d, it is obvious that there is a process of the period-doubling bifurcation in Fig. 10e. It indicates that in the annular liquid pool with a shallow liquid layer, the transition form of oscillations is from local to global oscillations, and the time nodes in the transition of the temperature oscillation are not consistent in different regions of the shallow liquid layer.

Conclusions

In this paper, we systematically investigate the characteristics of oscillations in annular liquid layers and obtained three main transition routes of temperature oscillations and surface oscillations: quasi-periodic bifurcations, period-doubling bifurcations accompanied with quasi-periodic bifurcations and tangent bifurcations accompanied with quasi-periodic bifurcations. In the annular liquid pool, the flow will transfer to the quasi-periodic bifurcation state with two fundamental frequencies soon after the periodic oscillation state. The complete path of the quasi-periodic oscillation transition is obtained: the periodic oscillation state- the quasi-periodic oscillation state with two fundamental frequencies- the quasi-periodic state with three fundamental frequencies- the aperiodic oscillation state. Besides, the transition route of the period-doubling bifurcation or tangent bifurcation is always accompanied by quasi-periodic bifurcations at the same time.

Meanwhile, the relationship between temperature oscillations at different positions in the annular liquid layer and the relationship between transition routes of the temperature oscillation and the free surface oscillation are also studied. In the ground environment, because of the coupling effect of buoyancy and surface tension, oscillation modes at different positions in the annular liquid layer are not exactly in time synchronization. The propagation path of the temperature oscillation is consistent with that of the displacement oscillation at the same point. Moreover, the locations of bifurcations in the annular liquid layer are random and the transition form of oscillations in the annular liquid layer is from local to global oscillations.

Acknowledgments This work is funded by Joint fund of National Natural Science Foundation of China: Study on the oscillations, transition routes and volume effects of thermocapillary convection (U1738116), Chinese Academy of Sciences: SJ-10 Satellite Program under grant No. XDA04020405 and XDA04020202-05, and China Manned Space Engineering program (TG-2).

References

Benz, S., Hintz, P., Riley, R.J., Neitzel, G.P.: Instability of thermocapillary–buoyancy convection in shallow layers. Part 2. Suppression of hydrothermal waves. J. Fluid Mech. **5**(359), 165–180 (2000)

Broze, G., Hussain, F.: Transitions to chaos in a forced jet: Intermittency, tangent bifurcations and hysteresis. J. Fluid Mech. **311**(311), 37–71 (1996)

Bucchignani, E., Stella, F.: Rayleigh-Benard convection in limited domains: part 2—transition to chaos. Num. Heat Transf. Part A—Appl. **36**(1), 17–34 (1999)

Chen, Z.-W., Li, Y.-S., Zhan, J.-M.: Double-diffusive Marangoni convection in a rectangular cavity: onset of convection. Phys. Fluids **22**, 034106 (2010)

Delbourgo, R., Kenny, B.G.: Universal features of tangent bifurcation. Aust. J. Phys. **38**(1), 1–22 (1985)

Gollub, J.P., Benson, S.V.: Many routes to turbulent convection. J. Fluid Mech. **100**, 449–470 (1980)

Grebogi, C., Ott, E., Yorke, J.A.: Crises, sudden changes in chaotic attractors, and transient chaos. Phys. D Nonlinear Phenom. **7**(1–3), 181–200 (1983)

Hale, J.K.: Dynamics and bifurcations. Texts Appl. Math. **3**(2–3), 719–731 (1991)

Hu, W.R., Tang, Z.M.: Floating Zone Convection in Crystal Growth Modeling. Science Press, Beijing (2003)

Jakeman, E., Hurle, D.T.J.: Thermal oscillations and their effect on solidification processes. Rev. Phys. Technol. **3**(1), 3 (1972)

Jiang, H., Duan, L., Kang, Q.: A peculiar bifurcation transition route of thermocapillary convection in rectangular liquid layers. Exp. Thermal Fluid Sci. **88**, 8–15 (2017a)

Jiang, H., Duan, L., Kang, Q.: Instabilities of thermocapillary-buoyancy convection in open rectangular liquid layers. Chin. Phys. B **26**(11), 316–323 (2017b)

Li, Y.-S., Chen, Z.-W., Zhan, J.-M.: Double-diffusive Marangoni convection in a rectangular cavity: transition to chaos. Int. J. Heat Mass Transf. **53**(23/24), 5223–5231 (2010)

Mukutmoni, D., Yang, K.T.: Rayleigh-Benard convection in a small aspect ratio enclosure 2. Bifurcation to chaos. J. Heat Transf.—Trans. ASME **115**(2), 367–376 (1993)

Mukutmoni, D., Yang, K.T.: Thermal-convection in small enclosures—an atypical bifurcation sequence. Int. J. Heat Mass Transf. **38**(1), 113–126 (1995)

Napolitano, L.G., Monti, R., Russo, G.: Some results of the Marangoni free convection experiment. In: European Symposium on Material Sciences under Microgravity, pp. 15–22 (1984)

Ostrach, S.: Low-gravity fluid flows. Ann. Rev. Fluid Mech. **14**(1), 313–345 (1982)

Peng, Z., Bin, Z., Li, D., Qi, K.: Characteristics of surface oscillation in thermocapillary convection. Exp. Thermal Fluid Sci. **35**, 1444–1450 (2011)

Peng, Z., Li, D., Qi, K.: Transition to chaos in thermocapillary convection. Int. J. Heat Mass Transf. **57**, 457–464 (2013)

Schwabe, D., Möller, U., Schneider, J., Scharmann, A.: Instabilities of shallow dynamic thermocapillary liquid layers. Phys. Fluids A Fluid Dyn. **4**(1992), 2368–2381 (1992)

Schwabe, D., Zebib, A., Sim, B.C.: Oscillatory thermocapillary convection in open cylindrical annuli. Part 1. Experiments under microgravity. J. Fluid Mech. **491**(491), 239–258 (2003)

Shi, W., Imaishi, N.: Hydrothermal waves in differentially heated shallow annular pools of silicone oil. J. Cryst. Growth **290**(1), 280–291 (2006)

Shi, W., Ermakov, M.K., Li, Y.R., et al.: Influence of buoyancy force on thermocapillary convection instability in the differentially heated annular pools of silicon melt. Micrograv. Sci. Technol. **21**(1), 289–297 (2009)

Sim, B.C., Zebib, A., Schwabe, D.: Oscillatory thermocapillary convection in open cylindrical annuli. Part 2. Simulations. J. Fluid Mech. **491**(491), 259–274 (2003)

Smith, M.K., Davis, S.H.: The instability of sheared liquid layers. J. Fluid Mech. **121**(121), 187–206 (1982)

Stella, F., Bucchignani, E.: Rayleigh-Benard convection in limited domains: Part 1—Oscillatory flow. Num. Heat Transf. Part A-Appl. **36**(1), 1–16 (1999)

Yan, A., Li, K., Tang, Z.M., Cao, Z.H., Hu, W.R.: Period-doubling bifurcations of the thermocapillary convection in a floating half zone. Sci. China Phys. Mech. Astron. **53**(9), 1681–1686 (2010)

Yasnou, V., Gaponenko, Y., Mialdun, A., et al.: Influence of a coaxial gas flow on the evolution of oscillatory states in a liquid bridge. Int. J. Heat Mass Transf. **123**, 747–759 (2018)

Yu, J.J., Wu, C.M., Li, Y.R., Chen, J.C.: Thermal-solutal capillary-buoyancy flow of a low prandtl number binary mixture with a -1 capillary ratio in an annular pool. Phys. Fluids **28**(8), 55 (2016)

Zhang, L., Luo, J.Q., Wu, C.M., Yu, J.J., Li, Y.R.: Thermocapillary convection in a binary mixture with moderate prandtl number in a shallow annular pool. Micrograv. Sci. Technol. **30**(1–2), 33–42 (2018)